

# Reconsidering the possibility of room temperature ferromagnetism in Mn doped Zirconium oxide

Akash Chakraborty\*

*Institut für Theoretische Festkörperphysik,  
Karlsruhe Institute of Technology, 76128 Karlsruhe, Germany and  
School of Engineering and Science, Jacobs University Bremen,  
Campus Ring 1, 28759 Bremen, Germany*

Georges Bouzerar†

*Institut Lumière Matière, Université Lyon 1-CNRS,  
F-69622 Villeurbanne Cedex, France*

(Dated: November 9, 2018)

## Abstract

The possibility to induce long range ferromagnetic order by doping oxides with transition metal ions has become a very exciting challenge in the last decade. Theoretically, it has been claimed that Mn doped  $\text{ZrO}_2$  could be a very promising spintronic candidate and that high critical temperatures could be already achieved even for a low Mn concentration. Some experiments have reported room temperature ferromagnetism (RT-FM) whilst some others only paramagnetism. When observed, the nature of RT-FM appears to be controversial and not clearly understood. In this study, we propose to clarify and shed light on some of these existing issues. A detailed study of the critical temperatures and low energy magnetic excitations in Mn doped  $\text{ZrO}_2$  is performed. We show that the Curie temperatures were largely overestimated previously, due to the inadequate treatment of both thermal and transverse fluctuations, and disorder. It appears that the Mn-Mn couplings can not explain the observed RT-FM. We argue, that this can be attributed to the interaction between large moments induced in the vicinity of the manganese. This is similar to the non magnetic defect induced ferromagnetism reported in oxides, semiconductors and graphene/graphite.

PACS numbers: 75.47.Lx, 75.10.-b, 75.40.Gb

The possibility to trigger and control ferromagnetism in transition metal doped oxides such as the widely studied  $\text{ZnO}^{1-5}$ ,  $\text{TiO}_2^{6,7}$ ,  $\text{HfO}_2^{8,9}$ ,  $\text{ZrO}_2^{10-12}$ ,  $\text{In}_2\text{O}_3^{13-15}$  etc. has led to a huge development over these last years. These dielectric and transparent materials (large band gap) could unambiguously lead in the near future to a plethora of technological applications, in both areas of spintronics and opto-electronics, such as light emitting devices, magnetic sensors, detectors, ultra low-power memory devices etc. The interest in such materials has been growing tremendously during the last few years as demonstrated by the large amount of work found in the literature. However, from the fundamental point of view, many questions are still to be clarified. The often reported room temperature ferromagnetism in these diluted magnetic oxides (DMO) is not always well understood. Recent experimental studies on Co doped  $\text{ZnO}^{16}$  interestingly revealed the existence of nano-sized ferromagnetic Co clusters, leading to critical temperatures of  $\sim 300$  K. The spinodal decomposition (alternating regions of low and high concentration of magnetic impurities) has been suggested to be the probable reason for the high Curie temperatures observed in some of these diluted materials<sup>17-19</sup>. Nevertheless, the fact remains that the nature and origin of the ferromagnetism is often controversial and not always systematically reproducible in most of the DMO. From this point of view the case of  $\text{ZrO}_2$ , also known as synthetic diamond, is particularly interesting.

In a recent letter<sup>20</sup>, the authors have predicted that the cubic zirconia could exhibit relatively high Curie temperatures (beyond 500 K) when doped with a relatively low concentration of Mn. It has also been shown that the ferromagnetism is robust against oxygen vacancies and defects. These interesting results have motivated many experimental studies. Unfortunately, many have failed to observe ferromagnetism or could not reproduce the results from other groups. The ferromagnetism, when observed, appears to be metastable and sensitive to the growth and preparation conditions. Very often a non-ferromagnetic phase in Mn-doped  $\text{ZrO}_2$  has been reported<sup>8,21,22</sup>. On the other hand, an inhomogeneous ferromagnetic phase has also been reported in zirconia thin films<sup>28</sup>. The observed phase appeared to be independent of the Mn concentration and was attributed to intrinsic defects. In other words they have concluded that the Mn ions play a secondary role in the latter case, which contradicts the theoretical predictions. More recently, high Curie temperature ferromagnetism in cubic Mn-doped  $\text{ZrO}_2$  thin films has been reported<sup>11</sup>. In this study, the authors have concluded that the ferromagnetism should result from the Mn-Mn exchange

interactions. This in our view is not convincing since for a Mn concentration of about 5% a huge moment of the order of  $13.8 \mu B$  per Mn was measured. In addition, in the monoclinic case room temperature ferromagnetism has also been observed in both doped and undoped host material. The conclusion was that in the latter case the FM is due to both the Mn-Mn couplings and the intrinsic defects. These defects were identified as structural defects, such as vacancies, located at the interface between film and substrate or at the surface. But the possibility of oxygen vacancies was ruled out from annealing measurements. Ferromagnetism can indeed be induced by non-magnetic or intrinsic defects, this phenomenon is also known as  $d^0$  ferromagnetism<sup>23-27</sup>. The non-trivial underlying physics involves many body aspects and still remains highly debated. In particular the competition between localization and electron-electron interaction which is at the origin of the magnetic moment formation in the vicinity of the defects. The induced moments could then eventually interact favorably, under certain conditions, and lead to long range ferromagnetic order.

In this letter, we propose to clarify the role of Mn-Mn couplings in cubic Mn-doped  $ZrO_2$ , and show that this exchange mechanism can not explain the room temperature ferromagnetism observed. We demonstrate that the high Curie temperature predicted in a previous theoretical study<sup>20</sup> originates from an inaccurate treatment of both disorder (percolation effects not included) and thermal fluctuations (underestimated). For instance, we find that in the 5% doped  $ZrO_2$ , the Curie temperature can not exceed 20 K. In addition, we present a detailed analysis of the nature of the magnetic excitations in defect free Mn doped zirconia. In the light of the current study, we will reconsider the interpretation of some existing experimental data.

The Hamiltonian describing  $N_{imp}$  interacting spins randomly distributed on a lattice of  $N$  sites is given by the diluted random Heisenberg model,

$$H_{Heis} = - \sum_{i,j} J_{ij} p_i p_j \mathbf{S}_i \cdot \mathbf{S}_j \quad (1)$$

where the sum  $ij$  runs over all sites and the random variable  $p_i$  is 1 if the site is occupied by an impurity, otherwise it is 0.  $\mathbf{S}_i$  is the localized  $Mn^{2+}$  spin at site  $i$ . The couplings  $J_{ij}$  depend on the Mn concentration<sup>29</sup> and have been calculated from *ab initio* method (Tight binding linear muffin tin orbitals). These couplings were used in Ref.20. The above Hamiltonian (Eq.1) is treated within the self-consistent local random phase approximation (SC-LRPA)<sup>30</sup>. It is a semi-analytical approach based on finite temperature Green's functions. This approach has

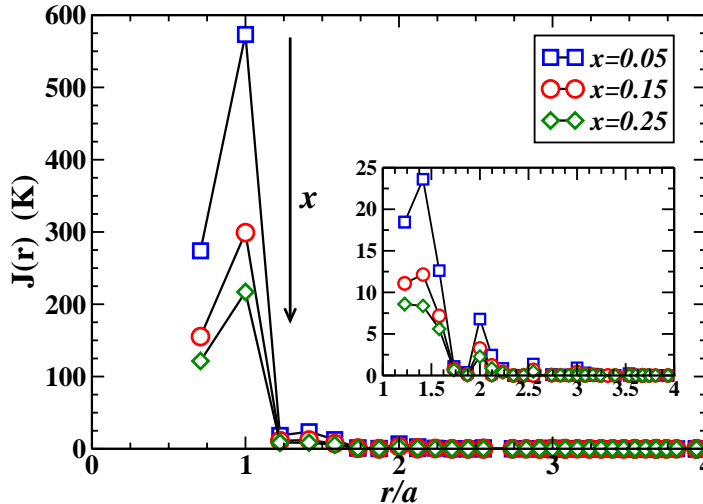


FIG. 1: (Color online) Mn-Mn magnetic couplings in units of K in Mn doped  $\text{ZrO}_2$  for various Mn concentrations  $x$ . The inset is a zoom of the extended exchange integrals<sup>29</sup>.

been discussed in details and implemented successfully several times in the past (for more details see Ref.31). The agreement obtained with other approaches such as Monte Carlo simulations<sup>32,33</sup> or site percolation statistics on random resistor networks<sup>34</sup> has established the reliability and accuracy of the SC-LRPA.

In Fig.1 , the Mn-Mn couplings for three different concentrations of Mn are plotted as a function of Mn-Mn distance. We observe that the couplings are all ferromagnetic but of very short range, beyond  $r = 2a$  they are almost negligible. Besides the first two couplings which are relatively large, the others are much smaller. The short ranged nature of the couplings already suggests that the percolation effects are expected to play a crucial role. Note that these magnetic couplings were obtained within a standard Local Density Approximation (LDA) approach. Although it is well known that LDA often leads to incorrect results in both oxides and strongly correlated systems<sup>35</sup>, we do not believe that the range of the couplings would drastically change with an improved treatment of the electronic correlations and thus affect qualitatively the nature of our conclusions.

In Fig. 2 we show the magnon density of states (DOS)  $\rho(\omega)$  for three different concentrations of Mn: low, intermediate and relatively large concentration. First, we observe that the overall shape changes drastically as we increase the Mn concentration. For the lowest concentration one sees that the magnon DOS has a significant weight only in the

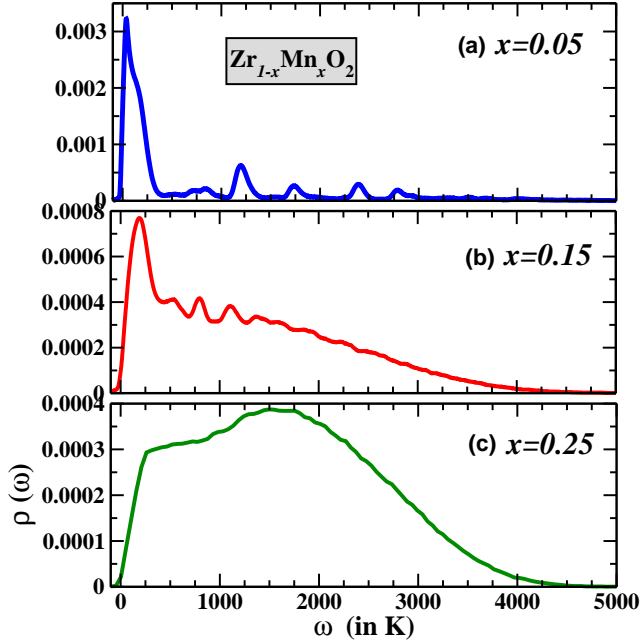


FIG. 2: (Color online) Average magnon density of states (DOS) at  $T=0$  K, corresponding to low, intermediate and large Mn concentrations: (a)  $x=0.05$ , (b)  $x=0.15$  and (c)  $x=0.25$ . The energy ( $x$  axis) is in unit of K.

relatively low energy region. In addition it exhibits a multiple peak structure separated by “pseudo gap” regions (very low density of states). These peaks result from weakly coupled clusters of Mn. Indeed, as seen previously both the nearest and next-nearest neighbor couplings are much larger than the others. For  $x = 0.15$  the magnon DOS has already changed significantly. Besides a relatively narrow peak at low energy the magnon DOS now has a significant weight which extends to relatively high energies. We still observe some peak structure for the intermediate energies. For the largest concentration  $x = 0.25$ , the magnon DOS exhibits now a broad peak at 1500 K and a flat region between 250 K to 1000 K. The significant change in the DOS when the Mn concentration varies from  $x = 0.15$  to  $x = 0.25$ , is a signature of the very short ranged nature of the exchange interactions.

Let us now discuss the effects of a proper treatment of both disorder and thermal/transverse fluctuations on the Curie temperatures, which is depicted in Fig.3. We compare the self-consistently calculated  $T_C$  to that given in Ref.20 which was obtained within the mean-field virtual crystal approximation (VCA). Its expression reads  $T_C^{VCA} = \frac{2}{3}x \sum_i z_i J_{0i}$ , where the sum runs over the shells and  $z_i$  denotes the number of sites on the  $i$ -th shell. First we observe that the critical temperatures obtained within SC-LRPA are much smaller. In

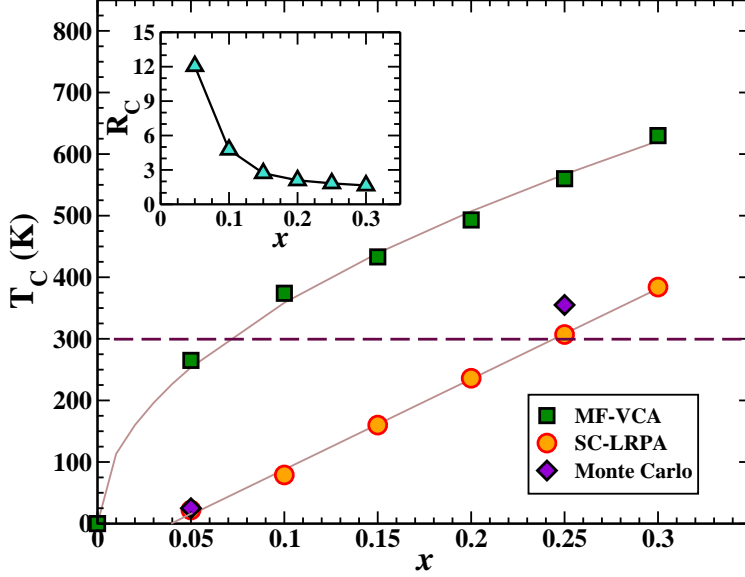


FIG. 3: (Color online) Curie temperature as a function of the Mn concentration  $x$ , calculated within (i) Mean Field VCA approximation (see text), (ii) SC-LRPA and (iii) Monte Carlo<sup>36</sup>. For SC-LRPA calculations the size of the symbols provides the error bar. The continuous lines are a guide to the eye. The inset is the ratio  $R_C = \frac{T_C^{VCA}}{T_C^{LRPA}}$ .

fact for 5% of Mn,  $T_C^{VCA}$  is 1200% larger than the true critical temperature, it is about 500% larger for 10% of Mn and it is two times larger even for 20% of Mn. Note that the SC-LRPA  $T_C$  is also in very good agreement with the Monte Carlo calculations<sup>36</sup>. While, within mean field,  $T_C$  beyond room temperature can be already achieved for only 5% of Mn, when disorder and thermal fluctuations are properly included room temperature ferromagnetism is only possible beyond 25% of Mn. The artificially high critical temperatures obtained within mean field is a consequence of the large values of the nearest and next nearest neighbor couplings, depicted in Fig.1. However, when the percolation effects are taken into account these couplings are expected to play only a negligible role in the dilute regime<sup>37</sup>. Note that  $T_C$  is well described by  $A(x - x_c)$ . This is in contrast to what was found for Mn-doped GaAs, where the best fit was of the form  $A'(x - x_c)^{1/2}$  (Ref.38). We believe that the origin of the linear like behavior in the present case arises from the strong dependence of the relevant couplings, for  $r/a \geq 1$ , on  $x$  (see Fig.1); unlike in the case of Mn-doped GaAs, where the typical couplings which controls the critical temperature were found to vary weakly with  $x$ .

These results clearly show that the room temperature ferromagnetism observed in about

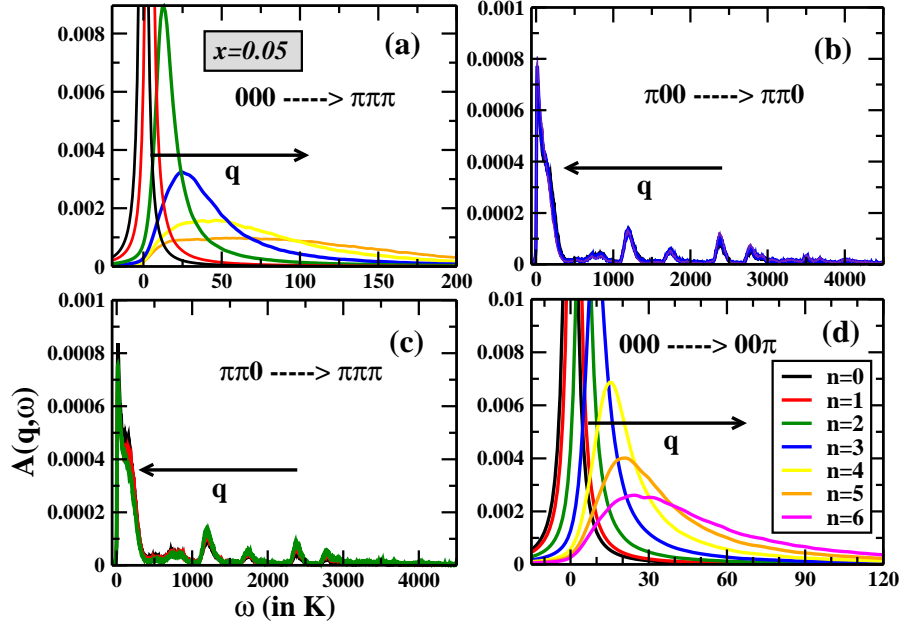


FIG. 4: (Color online) Spectral function averaged over the disorder  $A(\mathbf{q}, \omega)$  for different directions of the Brillouin zone. In each case, we show only few values of  $\mathbf{q}$ . In (a) and (d) only the lowest  $\mathbf{q}$  values are shown starting from the  $\Gamma$  point. In (d) the momentum correspond to  $\mathbf{q}=(0, 0, \frac{2\pi n}{La})$  where  $n=0,1,2,\dots,6$ . The Mn concentration is set to  $x=0.05$ . The system contains  $N = 4L^3$  sites where  $L=32$ .

5% Mn doped cubic  $\text{ZrO}_2$  reported in Ref.11 can not result from Mn-Mn couplings, in case of homogeneous distribution of dopants. The Mn-Mn exchange couplings mechanism would only lead to a critical temperature of about 20 K. We believe that the room temperature ferromagnetism observed in cubic Mn-doped zirconia could be of  $d^0$  nature<sup>23-27</sup>. The localized spin of  $\text{Mn}^{2+}$  plays an irrelevant role. The substitution of  $\text{Zr}^{4+}$  by  $\text{Mn}^{2+}$  would lead to the formation of large magnetic moments around the Mn-atoms, interacting with each other ferromagnetically via relatively extended couplings. This scenario would be consistent with the large moment of  $13.8 \mu B$  measured in Ref.11. Another possibility for the room temperature phenomenon observed in this case might be the presence of spinodal decomposed or inhomogeneous phases. However, a more careful and detailed structural analysis of the samples is necessary to confirm this scenario.

We now analyze the nature of the magnon excitations, with a particular focus on the

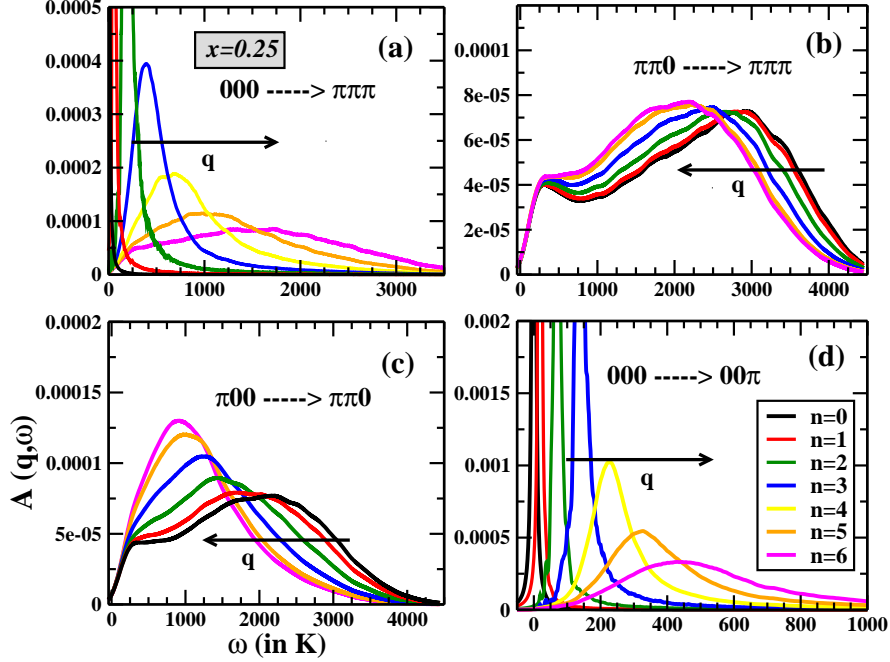


FIG. 5: (Color online) As in the previous figure, spectral function averaged over the disorder  $A(\mathbf{q}, \omega)$  for different directions of the Brillouin zone. The Mn concentration is set to  $x=0.25$ . The system contains  $N = 4L^3$  sites where  $L=20$ .

long wavelength limit. In Fig.4 we have plotted, for a fixed concentration of 5% of Mn and at  $T=0$  K the spectral function averaged over disorder. It is given by the following expression  $A(\mathbf{q}, \omega) = -\langle \frac{1}{2\pi S} \text{Im}G(\mathbf{q}, \omega) \rangle_c$ , where  $G(\mathbf{q}, \omega)$  is the Fourier transform of the retarded Green's function  $G_{ij}(t) = -i\theta(t)\langle [S_i^+(t), S_j^-(0)] \rangle$ , ( $\langle \dots \rangle$  denotes the thermal average and  $\langle \dots \rangle_c$  the average over disorder configurations). Fig.4(a)-(d) represent  $A(\mathbf{q}, \omega)$  in various directions in the Brillouin zone (BZ). We observe in (a) and (d) that well-defined magnons are visible only in a very narrow region around the  $\Gamma$  point. The width of the excitations is found to increase strongly as we move away from the  $\Gamma$  point. In (b) and (c) we observe that  $A(\mathbf{q}, \omega)$  is insensitive to the momentum. For these momenta,  $A(\mathbf{q}, \omega)$  is identical to the density of states shown in Fig.2. The magnon excitations are completely incoherent in these regions of the BZ. This behavior also indicates that these high energy modes (peaks) are completely localized. In Fig.5, the disorder averaged spectral function is now plotted for a larger concentration of Mn,  $x = 0.25$ . Qualitatively this figure resembles the previous one, besides the fact that the long wavelength modes are now well defined for a broader range of momentum  $q$  (the system size was  $L=32$  in Fig.4 and  $L=20$  in the present case). We will



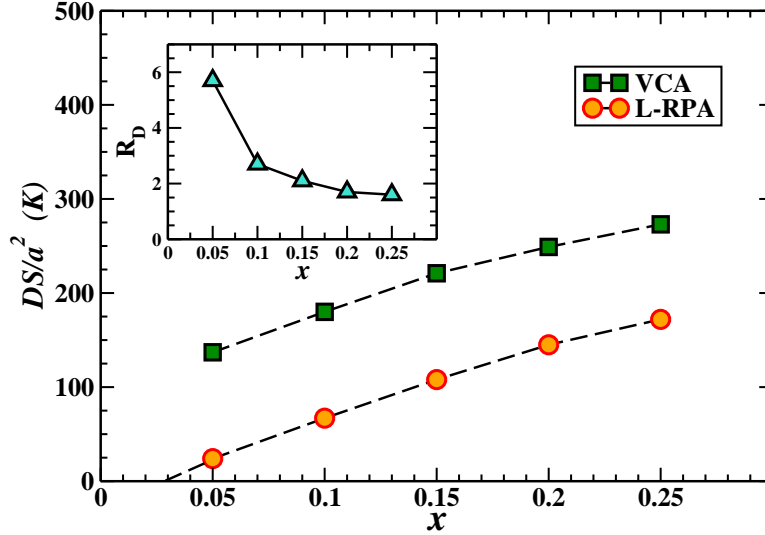


FIG. 6: (Color online) Averaged spin stiffness  $D$  as a function of the Mn concentration  $x$  in Mn doped  $\text{ZrO}_2$ . The calculations were performed both within VCA and SC-LRPA. The inset is the ratio  $R_D = \frac{D^{\text{VCA}}}{D^{\text{LRPA}}}$ .  $a$  is the lattice parameter.

come back to this point in a more quantitative way in what follows. In both (b) and (c), and in contrast to the low concentration case, we now observe a clear strong  $q$  dependence of  $A(\mathbf{q}, \omega)$ , more pronounced in (c). This indicates that the nature of the high energy modes differs from those seen in the low concentration case. However, even for this reasonably large concentration no well defined magnons exist in these regions of the BZ.

In order to get a better insight of the low energy excitations we have plotted in Fig.6 the spin stiffness  $D$  as a function of the Mn concentration. We remind that in the long wavelength limit the magnon energy scales like  $\omega(\mathbf{q}) = Dq^2$ . To evaluate quantitatively the effects of percolation and thermal fluctuations, both the mean field value and that calculated from the finite size analysis of  $A(\mathbf{q}, \omega)$  are shown. Note that the mean-field value of the spin stiffness is  $D^{\text{VCA}} = \frac{1}{3S} x \sum_i z_i r_i^2 J_{0i}$ , where the sum runs over the shells and  $r_i$  is the distance between the sites of the  $i$ -th shell and a site at the origin. We observe a dramatic effect on  $D$  for the low concentrations. Indeed, for  $x = 0.05$  the mean field spin stiffness is six times larger than that obtained within the local RPA. Even for the 10% doped system it is almost three times larger, and twice in the 20% case. We also observe that the extrapolation of

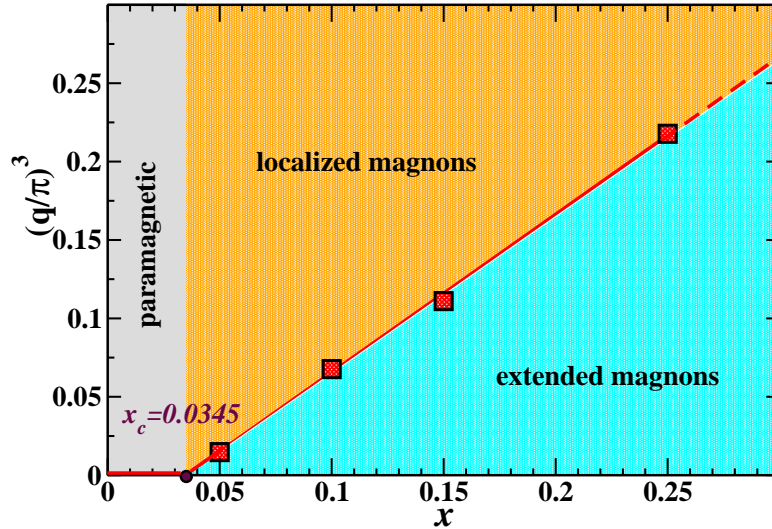


FIG. 7: (Color online) Phase diagram for the low energy magnon excitations. The symbols separate the extended well-defined magnon modes from the localized excitations (see text).  $x_c$  denotes the percolation threshold which is approximately 0.0345. Here we consider  $\mathbf{q}$  in the  $(1, 0, 0)$  direction.

the spin stiffness vanishes at approximately  $x \approx 0.03$  (percolation threshold). This agrees very well with the value that could be estimated from the critical temperature (Fig.3). We expect indeed, both  $T_C$  and  $D$  to vanish exactly at the percolation threshold.

Finally we provide a quantitative estimate of the region of the BZ where well defined magnons exist. We focus only in the  $(1,0,0)$  direction here. One way to extract accurately the critical line that separates extended from localized magnons would be to calculate the typical density of states<sup>39,40</sup>. This method allows to determine the mobility edge for the metal-insulator transition in the Anderson model. As this approach is more demanding, for the sake of simplicity, we consider the following alternative natural criterion: the magnon modes are well defined only if their linewidth  $\gamma(\mathbf{q})$  (inverse of the lifetime) is smaller than their energy  $\omega(\mathbf{q})$ . The results are depicted in Fig.7. We find that the line that separates the well defined magnons from localized magnon modes is given by  $q_c = A(x - x_c)^{1/3}$ , where  $x_c$  is found to be 0.0345. This is in excellent agreement with that extracted from the spin stiffness and the critical temperature. One immediately sees, for the 25% doped case the volume of well defined magnons is fifteen times larger than that of the 5% doped zirconia.

To conclude, we have shed light on some existing controversies on the origin of room

temperature ferromagnetism in Mn doped zirconia. We have demonstrated that the Mn-Mn interactions alone can not give rise to room temperature ferromagnetism in  $\text{ZrO}_2$ , in contrast to what was predicted in previous theoretical studies. In particular, it has been shown that the 5% Mn doped systems is close to percolation and its critical temperature can not exceed 20 K. Room temperature ferromagnetism is reachable only for large Mn concentration, beyond 25%. Thus, in our view, the room temperature ferromagnetism observed experimentally in cubic Mn-doped zirconia could be of  $d^0$  nature, and the spin of Mn plays only a secondary role. The question is whether the manganese induces large magnetic moment in its surrounding or the ferromagnetism is due to other intrinsic defects. However, we do not rule out the possibility of nanoscale spinodal decomposition which can also lead to room temperature ferromagnetism, even in the 5% doped case, for effective short-ranged interactions. It will be interesting to investigate these issues experimentally. In addition, we have presented a detailed analysis of the energy and linewidth of the spin excitations with a particular focus on the long wavelength limit (spin stiffness). It is found that for 5% doped zirconia extended magnons exist only within about 2% of the volume of the Brillouin zone, whilst it reaches approximately 25% for 25% doped zirconia. We believe that our study should also be relevant for other compounds, namely transition metal ion doped oxides such as  $\text{TiO}_2$ ,  $\text{HfO}_2$ ,  $\text{SnO}_2$  or  $\text{In}_2\text{O}_3$ .

### Acknowledgments

This work was supported by the EU within FP7-PEOPLE-ITN-2008, Grant number 234970 Nanoelectronics: Concepts, Theory and Modelling. We thank J. Kudrnovský for providing us with the Mn-Mn couplings in  $\text{ZrO}_2$ . We would also like to thank L. Bergqvist for the Monte Carlo data.

---

\* Electronic address: akash.chakraborty@physik.uni-regensburg.de

† Electronic address: georges.bouzerar@univ-lyon1.fr

<sup>1</sup> T. Fukumura et. al. Appl. Phys. Lett. **75**, 3366, (1999).

<sup>2</sup> K. Sato and K. Yoshida, Jpn. J. Appl. phys. **40**, L334 (2001).

<sup>3</sup> J. H. Kim, J. Appl. Phys. **92**, 6066 (2002).

- <sup>4</sup> P. Sharma et al. *Nat. Mat.* **2**, 673 (2003).
- <sup>5</sup> L. M. C. Pereira et al. *J. Appl. Phys.* **113**, 023903 (2013).
- <sup>6</sup> G. Glaspell, A. B. Panda, and M. S. El-Shall, *J. Appl. Phys.* **100**, 124307 (2006).
- <sup>7</sup> L. A. Errico, M. Renteria, and M. Weissmann, *Phys. Rev. B* **72**, 184425 (2005).
- <sup>8</sup> A. Pucci, G. Clavel, M-G. Willinger, D. Zitoun, and N. Pinna, *J. Phys. Chem. C* **113**, 12048 (2009).
- <sup>9</sup> N. H. Hong, J. Sakai, N. Poirot, and A. Ruyter, *Appl. Phys. Lett.* **86**, 242505 (2005).
- <sup>10</sup> J. M. D. Coey, M. Venkatesan, P. Stamenov, C. B. Fitzgerald, L. S. Dorneless, *Phys. Rev. B* **72**, 024450 (2005).
- <sup>11</sup> N. H. Hong, C.-K. Park, A. T. Raghavender, O. Ciftja, N. S. Bingham, M. H. Phan, and H. Srikanth, *J. Appl. Phys.* **111**, 07C302 (2012).
- <sup>12</sup> D. Sangalli et al. *Eur. Phys. J. B* **86**, 211 (2013).
- <sup>13</sup> N. H. Hong et al. *Phys. Rev. B* **73**, 132404 (2006).
- <sup>14</sup> J. Phillip et al. *Appl. Phys. Lett.* **85**, 777 (2004).
- <sup>15</sup> G. Peleckis, X. Wang, and X. D. Shi, *Appl. Phys. Lett.* **89**, 022501 (2006).
- <sup>16</sup> N. Jedrecy, H. J. von Bardeleben, and D. Demaille, *Phys. Rev. B* **80**, 205204 (2009).
- <sup>17</sup> H. Katayama-Yoshida et. al. *Phys. Stat. Sol. (a)* **204**, 15 (2007).
- <sup>18</sup> A. Bonanni and T. Dietl, *Chem. Soc. Rev.* **39**, 528 (2010).
- <sup>19</sup> A. Chakraborty, R. Bouzerar, S. Kettemann, and G. Bouzerar, *Phys. Rev. B* **85**, 014201 (2012).
- <sup>20</sup> S. Ostanin, A. Ernst, L. M. Sandratskii, P. Bruno, M. Dane, I. D. Hughes, J. B. Staunton, W. Hergert, I. Mertig, and J. Kudrnovský, *Phys. Rev. Lett.* **98**, 016101 (2007).
- <sup>21</sup> G. Cravel, M.-G. Willinger, D. Zitoun, and N. Pinna, *Eur. J. Inorg. Chem.* 2008, **863**, (2008).
- <sup>22</sup> S.K. Srivastava, P. Lejay, B. Barbara, O. Boisron, S. Pailhes and G. Bouzerar, *J. Appl. Phys.* **110**, 043929 (2011).
- <sup>23</sup> I.S. Elfimov, S. Yunoki and G.A. Sawatzky, *Phys. Rev. Lett.* **89**, 216403 (2002).
- <sup>24</sup> J. Osorio-Guillen, S. Lany, S. V. Barabash, A Zunger, *Phys. Rev. Lett* **96**, 107203, 2006.
- <sup>25</sup> M. Venkatesan et al. *Nature (London)* **430**, 630 (2004), J.M.D. Coey et al., *Phys. Rev. B*, **72**, 024450 (2005).
- <sup>26</sup> P. Esquinazi et al. *Phys. Rev. Lett.*, **87**, 227201 (2003).
- <sup>27</sup> F. Maca, J. Kudrnovský, V. Drchal, and G. Bouzerar, *Appl. Phys. Lett.* **92**, 212503 (2008); G. Bouzerar and T. Ziman, *Phys. Rev. Lett.* **96**, 207602 (2006).

- <sup>28</sup> J. Zippel, M. Lorenz, A. Setzer, G. Wagner, N. Sobolev, P. Esquinazi, and M. Grundmann, Phys. Rev. B **82**,125209 (2010).
- <sup>29</sup> J. Kudrnovský, *private communication*.
- <sup>30</sup> G. Bouzerar, T. Ziman, and J. Kudrnovský, Europhys. Lett. **69**, 812 (2005).
- <sup>31</sup> K. Sato et. al., Rev. Mod. Phys. **82**, 1633 (2010).
- <sup>32</sup> L. Bergqvist, O. Eriksson, J. Kudrnovský, V. Drchal, P. Korzhavyi and I. Turek, Phys. Rev. Lett. **93**, 137202 (2004).
- <sup>33</sup> G. Bouzerar and O. Cepas, Phys. Rev. B **76**, 020401R (2007).
- <sup>34</sup> A. Chakraborty and G. Bouzerar, Phys. Rev. B **81**, 172406 (2010).
- <sup>35</sup> see for example A. Zunger, S. Lany, and H. Raebiger, Physics **3**, 53 (2010).
- <sup>36</sup> L. Bergqvist, *private communication*.
- <sup>37</sup> R. Bouzerar and G. Bouzerar, New J. of Physics **12**, 053042 (2010).
- <sup>38</sup> G. Bouzerar, T. Ziman, and J. Kudrnovský, Phys. Rev. B **72**, 125207 (2005).
- <sup>39</sup> V. Dobrosavljević, A. A. Pastor, and B. K. Nikolic, Europhys. Lett. **62**, 76 (2003).
- <sup>40</sup> V. Dobrosavljević and G. Kotliar, Phys. Rev. Lett. **78**, 3943 (1997).